Energy Technology
Generation, Conversion, Storage, Distribution
www.entechnol.de

Electricity Arbitration and Sector Coupling with an Experimentally Validated Reversible Solid Oxide Cell Reactor System Connected to the Natural Gas Grid

Srikanth Santhanam, Marc P. Heddrich, and Kasper Andreas Friedrich*

Chemical energy storage offers an attractive solution for the arbitration of intermittent renewable electricity due to its higher energy storage capacity and storage duration. Reversible solid oxide cell (rSOC) reactor systems can efficiently operate in electrolysis operation to convert electrical energy to chemical energy or in fuel cell mode to convert chemical energy back to electrical energy. Natural gas is widely used in the chemical industry as a source of energy and hydrogen. Hence, storing electrical energy in the form of synthetic natural gas can couple electricity arbitration with chemical process industries. A methane-based rSOC system concept for the purpose of energy storage and sector coupling is investigated. A process system analysis is performed based on an experimental study of a commercially available rSOC reactor. A validated rSOC reactor model is used to identify optimal system operating conditions. The proposed system concept achieves a chemical to electrical energy conversion efficiency of 57% and electrical to chemical energy conversion efficiency of 93% based on first law and lower heating value. A net electrical storage efficiency of 53% can be achieved.

1. Introduction

Efficient energy storage and management systems are required for a successful transition to a renewable-energy-powered society. They are necessary to balance the temporal variations of the renewable energy supply (such as wind and solar) with the time-varying nature of the energy demand.[1] Storing electrical energy in chemical fuels (either in gaseous or liquid form) is very attractive and beneficial due to high storage capacity.[2,3] Additionally, by moving toward a defossilized society driven by renewable energy where electrical energy becomes a prime mover, new pathways are needed to produce essential chemical energy and important industrial chemicals.[4] Hence, this provides an opportunity to combine energy storage with chemical synthesis in industrial applications. Electrical energy from renewable sources can be used to produce hydrogen or syngas by the process of electrolysis which can be further converted to high value chemical fuels. Solid oxide cell (SOC) electrochemical reactors are especially attractive due to their high efficiency compared with other electrochemical reactors. The high operation temperature (typically above 700 °C) reduces the electrochemical losses[5–8] and enables faster kinetics. The oxide-ion-conducting electrolyte enables it to operate as both solid oxide fuel cell (SOFC) and solid oxide electrolysis cell (SOEC) reactor. In electrolysis process, the SOCs can electrolyze steam and carbon-dioxide simultaneously commonly referred to as coelectrolysis.[9,10] Under appropriate conditions, methane can also be produced within the SOC reactor during coelectrolysis.[11] This bidirectional functionality for the SOC electrochemical reactor systems enables the possibility to have energy-conversion systems that can operate in electrolysis mode to store electricity or in fuel-cell mode to produce electricity. Such systems are referred to as reversible Solid Oxide Cell (rSOC) systems.[12–14]

Dr. S. Santhanam, Dr. M. P. Heddrich, Prof. K. A. Friedrich
Institute for Engineering Thermodynamics
German Aerospace Center (DLR)
Pfaffenwaldring 38-40, 70569 Stuttgart, Germany
E-mail: srikanth.santhanam@dlr.de

Prof. K. A. Friedrich
Institute of Buildin Energetics
Thermal Engineering and Energy Storage (IGTE)
University of Stuttgart
Pfaffenwaldring 31, 70569 Stuttgart, Germany

The ORCID identification number(s) for the author(s) of this article can be found under https://doi.org/10.1002/ente.201900618.

DOI: 10.1002/ente.201900618

1.1. Motivation

Methane as a chemical has a huge industrial significance in both chemical process and energy industry. Hence, storing or converting excess electricity from renewable sources to synthetic methane is highly attractive. Moreover, methane can be fed directly to the existing natural gas grid and is therefore easily transportable.[15,16] Standalone power to methane systems using SOC reactors have been proposed by researchers.[17–19] Similarly, standalone SOFC systems running on methane/natural gas have been extensively studied and demonstrated.[20–22] In principle, the bidirectional operation of SOC reactor can enable an unitized rSOC system that can operate as both power-to-methane (SOEC) or methane-to-power (SOFC) system. The methane produced in power-to-methane mode can be used in fuel-cell mode for

efficient conversion to electricity when the renewable electricity supply is less than the demand. Conceptual studies of electricity storage in the form of methane using a unitized rSOC systems were proposed in literature. Bierschenk et al.[11] proposed the initial thermodynamic concept of a unitized rSOC system based on methane. Monti et al.[23] and Wendel et al.[24] extended the thermodynamic concept with a process system for a methane-based energy storage system using rSOC electrochemical reactors. In their work, they proposed a system based on a future SOC reactor with thin electrolytes and operation temperature of 600 °C which is still in early stages of development. They proposed a closed system concept where the methane is stored in gas tanks or in caverns. Mottaghizadeh et al.[25] proposed a methane-based energy storage system using a commercially available SOC reactor operating at temperature above 750 °C where an option of integrating heat storage for thermal management was suggested. The methane concentration of product gas was low and not sufficient for integrating with the natural gas grid. Finally, the all-reported literature on process system studies utilized a 0-D or black box model of the electrochemical reactor. This can often lead to overestimation of system performances or to operating conditions that would result in reactor failure due to local effects that black box models will not reveal. Li et al.,[26] Magistri et al.[27] and Oryshchyn et al.[28] showed that implementing a detailed reactor model, as compared with a 0-D model, in process system simulations significantly altered the system performance and certain operation points were deemed unfeasible. This is especially critical for an rSOC system where the SOC reactor will have to function in both operation modes.[29]

1.2. Scope

In this study, a unitized rSOC system is developed based on an experimentally characterized commercially available SOC reactor for energy storage and sector coupling. The proposed system aims to achieve product gas with high methane concentration (>90 mol%) during the electrolysis operation. This can be supplied to the natural gas grid or to other chemical industries. The proposed system can switch to fuel cell operation to produce electricity by consuming methane from the natural gas grid as a fuel. A methodology combining theoretical, experimental, and simulation methods for process system development was utilized. The proposed methodology simplifies the selection of process parameters, operation parameters of key components such as the rSOC reactor. The methodology ensures the operability of the rSOC reactor and the proposed system concept by using a 1-D reactor model of the rSOC reactor. An exergy analysis is performed to identify the source of exergy destruction and opportunities to improve the system performance.

1.3. Scientific Method

The scientific method is comprised of two phases. In the first phase, a thermodynamically ideal system model is used to determine the maximum achievable system performance. The ideal system has no irreversibilities and compares performance utilizing either an ideal electrochemical reactor or a currently available experimentally characterized reactor. The performance is purely dictated by thermodynamics and represents the highest theoretical efficiency that is thermodynamically feasible. Theoretical and experimental phase determines the limits of the system performance for the given reactor technology at different operation parameters such as temperature, pressure, current density, and conversion ratio. This determines the preferred operation window for the complete process system including the balance of plant (BoP) components. In the second step, mathematical models are developed detailed process system analysis including the BoP. A detailed process system simulation is performed to quantify the system performance. Operation points and system architectures that can lead to rSOC reactor failure are omitted. The final system architecture and operation parameters should ensure safe reactor operation, meaning no hot spots, steep temperature gradients, and so on.

2. Theoretical and Experimental Analysis

2.1. Theoretical Method Part

The theoretical analysis to evaluate the thermodynamic potential of the concept is performed by using an ideal system concept as shown in **Figure 1**. The ideal system concept considers only the thermodynamic implications of the first and second law. It does not consider the losses or entropy generation caused by irreversibilities occurring in heat, mass, and charge transport processes. The ideal system consists of an isothermal ideal rSOC reactor (with no electrochemical losses) operating at temperature T and pressure p. The reactants are supplied from storage tanks to the rSOC reactor at the reaction operation temperature and the products are cooled from reactor temperature to the storage tank temperature. The ideal heat recovery process for the preheating of the reactants and cooling of the products is implemented by a combination of ideal heat pump and heat engines. The nonideal behavior and losses can be implemented by assuming exergy efficiencies for heat engine and heat pumps. Thermodynamic conditions of the storage tanks are such that there is no condensation of water or phase changes. The heat produced due to exothermic fuel cell operation is stored in the heat storage which can be used for endothermic electrolysis operation. This implies that the reactor temperature during fuel cell operation (T_{fc}) is higher than the heat storage temperature (T_{hs}) which is higher than the reactor temperature in electrolysis operation (T_{ec}). A discussion of the adopted method is provided by Santhanam et al.[12]

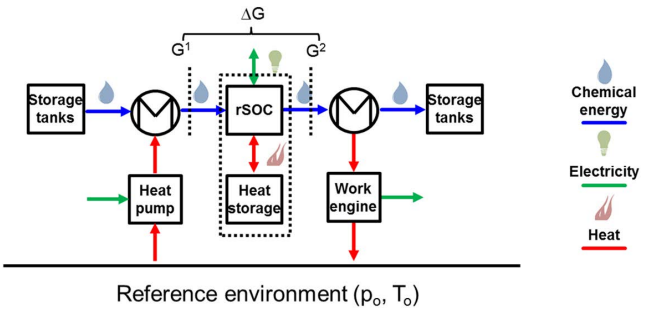

Figure 1. Schematic of ideal system concept for theoretical analysis.

$$T_{fc} > T_{hs} > T_{ec} \quad (1)$$

In fuel cell operation, a reactant fuel mixture primarily composed of hydrogen (H_2), methane (CH_4), and carbon monoxide (CO) is supplied to the rSOC reactor where it undergoes electrochemical oxidation. Electricity and heat are produced and products are mainly composed of water (H_2O) and carbon dioxide (CO_2) along with unreacted fuel mixture depending on the conversion ratio. In the electrolysis operation, the H_2O and CO_2 along with unreacted fuel is supplied to the rSOC reactor as reactants where electrochemical reduction occurs. Electrical energy and heat (depending on endothermic, thermo-neutral, or exothermic mode) is consumed by the reactor to produce fuel mixture. For the complete process, to have sufficient production of methane during the electrolysis process and to prevent carbon deposition problems in both SOFC and SOEC mode, an H/C/O ratio of 7/1/2 is required. Based on thermodynamic equilibrium study, a H/C ratio of 6–7 is required for methane formation in electrolysis mode[30] and a minimal O/C ratio of 2 is needed to prevent carbon deposition.[31–34] Additionally, the following assumptions are made to simplify the analysis.

1) The time period of reactor operation in fuel cell mode is equal to that of electrolysis mode.

$$t_{fc} = t_{ec} \quad (2)$$

2) The charge transferred during the discharge mode (fuel cell) is equal to the charge transferred during the charging mode (electrolysis).
3) Assumptions 1 and 2 imply that the current obtained from the SOC reactor in SOFC mode is equal in magnitude (but opposite in sign) to the current supplied to the SOC reactor in SOEC mode.

$$I_{fc} = I_{ec} \quad (3)$$

4) The product gases are assumed to reach thermodynamic equilibrium at the reactor outlet. The composition of the products are calculated based on chemical equilibrium.

2.2. Experimental Part

A commercially available rSOC reactor was used as a basis for this work. The rSOC reactor is based on the electrolyte-supported cell design with a 90 μm thick electrolyte made of 3 mol% Ytrria-stabilized Zirconia (3YSZ). The fuel electrode is a Nickel (Ni) cermet with gadolinium-doped ceria (GDC) and additionally has a nickel foam. The total thickness of the fuel electrode (along with nickel foam) is 30 μm. Finally, the air electrode is a perovskite, lanthanum-strontium-cobalt-ferrate (LSCF) and has a GDC-protective coating between the YSZ electrolyte and LSCF electrode. The total thickness of the air electrode is 55 μm. The performance of the commercial reactor was experimentally characterized at operation temperatures from 700 to 850 °C between 1.4 to 8 bar operation pressures. The experimental study was performed in both fuel cell and electrolysis operation. A detailed description of the experimental setup and methods provided in the literature by Riedel et al.[35] A detailed description of the theoretical model of the rSOC reactor and its validation is provided by the author in the literature.[12]

The electrochemical reactions, (R1a)–(R1b), oxidation of H_2 and CO during the fuel cell operation and reduction of H_2O and CO_2 during the electrolysis operation occurs at the fuel electrode. The reaction (R1c), occurs at the oxygen electrode. Apart from the electrochemical reactions at the fuel electrode, chemical reactions such as reverse water–gas shift (RWGS),(R3), and reverse steam reforming (SMR), (R2), reactions can occur under appropriate conditions as Ni is a good catalyst for these reactions at typical operation temperatures of the rSOC reactor. Reactions at the fuel electrode

$$H_2 + O^{2-} \rightleftharpoons H_2O + 2e^- \quad (R1a)$$

$$CO + O^{2-} \rightleftharpoons CO_2 + 2e^- \quad (R1b)$$

Reaction at the oxygen electrode

$$(1/2)O_2 + 2e^- \rightleftharpoons O^{2-} \quad (R1c)$$

$$CH_4 + H_2O \rightleftharpoons 3H_2 + CO \quad \Delta_r h = 206\,\text{kJ mol}^{-1} \quad (R2)$$

$$CO + H_2O \rightleftharpoons H_2 + CO_2 \quad \Delta_r h = -41\,\text{kJ mol}^{-1} \quad (R3)$$

The detailed description of the thermodynamic model of the rSOC reactor used for the theoretical analysis is presented by the author in the previous work.[12] A brief overview of the main equations are found in the Supporting Information.

2.3. Results and Discussion

2.3.1. Ideal Performance with and without Heat Storage

Roundtrip Efficiency without Heat Storage: The thermodynamic limit for the energy storage efficiency of the proposed concept can be discussed for two case; 1) without heat storage and 2) with heat storage. For the concept without heat storage, the electrical energy storage or the roundtrip efficiency for the theoretical system described earlier is defined as the ratio of the work produced during the fuel cell process to the total energy consumed by the reactor during the electrolysis process as shown in Equation (5). In the fuel cell more, the electric work produced by the reactor is equal ΔG (change in Gibbs energy) and total energy consumed by reactor during electrolysis corresponds to ΔH (change in enthalpy) of the process.

$$\eta_{RT} = \frac{W_{rev,fc}}{W_{rev,ec} + Q_{rev,ec}} \quad (4a)$$

$$\eta_{RT} = \frac{-\Delta G_{fc}}{\Delta H_{ec}} = \frac{-\Delta G_{fc}}{\Delta G_{ec} + T_{ec}\Delta S_{ec}} \quad (4b)$$

The variation of the roundtrip efficiency for different reactor temperatures and pressures is shown in **Figure 2**. In rSOC reactor, only the electrochemical reactions contribute to the work term (W_{rev}) in both fuel cell and electrolysis mode. The reactions, RWGS ((R3)) and SMR ((R2)), do not take part electrochemically and hence the work potential of these reactions is lost.[36,37]

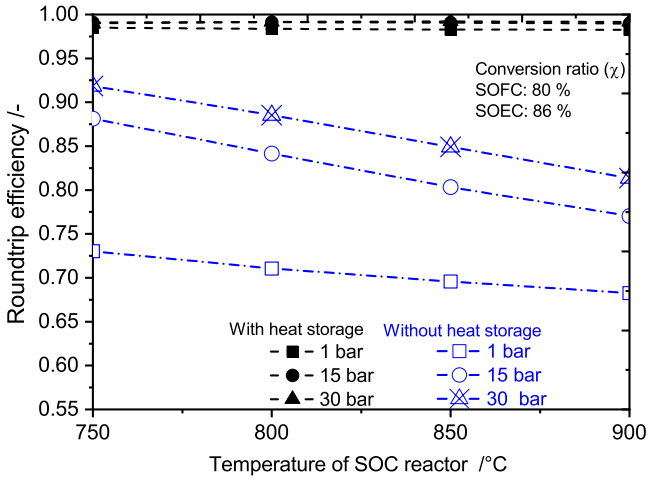

Figure 2. Variation of the roundtrip efficiency for rSOC system with and without heat storage for different pressures.

Therefore, theoretical work term (W_{rev}) in Equation (4a) is evaluated by Equation (5).

$$W_{rev,\,fc} = -(G^2 - G^1) - (-\Delta_{R2}G) \tag{5}$$

In the SOEC mode, the total energy to be supplied to the reactor corresponds to the total enthalpy change of the all reactions. For the rSOC system under consideration, the total energy input to the system is equal to the sum of enthalpy change of individual reactions (Equation (6)).

$$\Delta H_{ec} = \sum_i \Delta_{rxn,i} H, \quad i \in (\text{R1a}) - (\text{R3}) \tag{6}$$

To be more specific, the total enthalpy change of the electrolysis can be resolved to sum of electric work supplied to the reactor during electrolysis and heat supplied to the process.The heat input to the reactor is then the sum of heat required for endothermic electrochemical reactions, the exothermic chemical reaction of the SMR reaction, and slightly endothermic RWGS reaction. Accordingly, function roundtrip efficiency of the system with reactor temperature and pressure as observed in Figure 2 can be explained. As temperature increases, the electric work (ΔG of electrochemical reaction) decreases, whereas the heat ($T\Delta S$ part) for the electrochemical reaction increases, resulting in decreasing roundtrip efficiency with increasing reactor temperature. In electrolysis operation at high temperatures and low pressures, the enthalpy change is dictated predominantly by the endothermic electrochemical reduction of H_2O and CO_2 as exothermic methanation (reverse of (R2)) is not favored at high temperatures. As the system operation pressure is increased, it can be observed that the roundtrip efficiency increases significantly. As the pressure increases, the methane formation is favored via reverse of (R2) due to Le Chatelier's principle. First, H_2 and CO are produced by the electrochemical reactions in the electrolysis mode and the hydrogenation of CO to methane via reverse of reaction (R2) decreases the partial pressure of H_2 and CO, reducing the ideal voltage (and hence the ideal work) in the electrolysis mode. Second, due to increased rate of exothermic methanation reaction, the heat required by the reactor reduces greatly. This compounded effect significantly increases the roundtrip efficiency with pressure. At low temperatures and high pressure, the methanation reaction is thermodynamically most favorable. The roundtrip efficiency can be increased close to 100% by combining a heat storage such that the heat produced in the SOFC process is recirculated within the system during the electrolysis mode.

Roundtrip Efficiency with Heat Storage: When heat storage is considered and heat is stored within the control volume of the system, then the roundtrip efficiency is given by Equation (7) as the ratio of the net electric work produced during the fuel cell operation to the net electric work consumed during the electrolysis operation mode. The net electric work in fuel cell operation is the difference between the ideal work and work lost due to the losses. Similarly, in the electrolysis operation, the net work is the sum of ideal work and extra work to be supplied due to the losses.

$$\eta_{rt} = \frac{W_{fc}}{W_{ec}} \tag{7}$$

where

$$W_{fc} = (U_{id,fc} - \Delta U_{fc}) I_{fc} t_{fc} \tag{8}$$

$$W_{ec} = (U_{id,ec} + \Delta U_{ec}) I_{ec} t_{ec} \tag{9}$$

In the aforementioned equations, U_{id} denotes the ideal voltage given by the difference between the Gibbs function at the outlet and inlet of the rSOC reactor, subscript fc and ec indicates fuel cell and electrolysis operation, ΔU denotes the voltage loss due to the electrochemical losses. Hence, the for an ideal system with no losses, the theoretical maximum roundtrip efficiency is given by Equation (10)

$$\eta_{rt,id} = \frac{W_{fc}}{W_{ec}} = \frac{U_{id,fc} I_{fc} t_{fc}}{U_{id,ec} I_{ec} t_{ec}} \tag{10}$$

Furthermore, for the analysis, it is considered that the magnitude of temperature difference between the rSOC and heat storage is the same in both modes.

$$\Delta T = T_{fc} - T_{hs} = T_{hs} - T_{ec} \tag{11}$$

This implies:

$$2\Delta T = T_{fc} - T_{ec} \tag{12}$$

The theoretical roundtrip efficiency with heat storage is shown in Figure 2. With the heat storage, the efficiency is ratio of only the work terms. The roundtrip efficiency increases to 98% with heat storage but not 100%. This is due to the fact that the rSOC reactor temperature is lower in electrolysis operation than in fuel cell operation. Therefore, the work consumed during electrolysis is slightly higher than work produced during fuel cell mode.

2.3.2. Maximum Roundtrip Efficiency for Commercial rSOC Reactor

The maximum achievable efficiency for the given reactor is show in **Figure 3**. At a reactor temperature of 850 °C in SOFC mode and ΔT of 25 K (refer Equation (11) and (12), a roundtrip

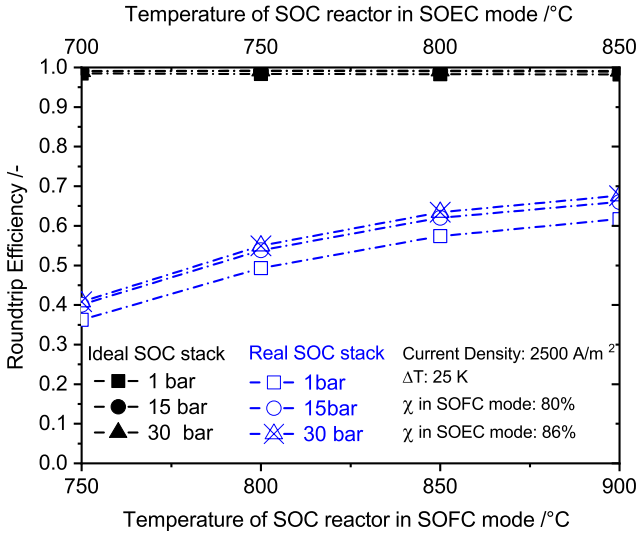

Figure 3. Comparison of roundtrip efficiency of an rSOC system with ideal reactor and commercial reactor conversion (χ) = 86% in SOEC mode and $\Delta T = 25$ K. $T_{fc} - T_{ec} = 2\Delta T$.

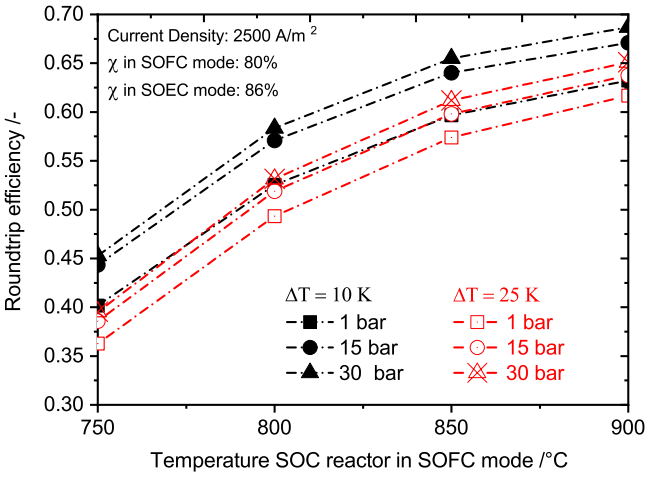

Figure 4. Impact of ΔT on roundtrip efficiency for the system with commercial reactor, conversion (χ) = 86% in SOEC mode. $T_{fc} - T_{ec} = 2\Delta T$.

efficiency of 55% is achievable at 1 bar pressure and 80% conversion in SOFC mode, whereas the theoretical maximum under the same conditions was shown to be around 98%. Therefore, the difference is purely due to the high losses in the current state-of-the-art reactor. The different electrochemical losses can be lumped to single term called the area specific resistance (ASR) in $\Omega\,cm^2$. ASR is a measure of reactor performance; the higher ASR implies higher losses and lower performance. For this rSOC reactor, ASR is largely dominated by the ohmic resistance to oxide-ion transport through the thick electrolyte. It contributes almost 80% of the total losses in the reactor. The readers are referred to Santhanam et al.[12] and Riedel et al.[35] for extended analysis of the results of SOFC and SOEC experiments, respectively. The ohmic resistance is a function of temperature and therefore the losses increases with decreasing temperature. Hence, the roundtrip efficiency decreases with decreasing temperature. The roundtrip efficiency falls to 35% at 750 °C. With improvements in rSOC reactor having lower ASR, the roundtrip efficiency can move toward ideal roundtrip efficiency. As pressure is increased, the roundtrip efficiency increases marginally. This behavior is purely due to the thermodynamics of the system. In the electrolysis operation mode, H_2 and CO are produced by the electrochemical reactions and the hydrogenation of CO to methane via reverse of reaction (R2) is favored with increasing pressure. The H_2 and CO partial pressure decreases which reduces the ideal voltage (and hence the ideal work) in the electrolysis mode due to the Nernst equation. Therefore, this results in a marginal increase in roundtrip efficiency with increasing pressure.

Impact of Temperature Difference Between rSOC Reactor and Heat Storage: The impact of the temperature difference between the rSOC reactor and heat storage is shown in **Figure 4**. Temperature difference between rSOC reactor and heat storage implies a temperature difference between two operation modes. A temperature difference of 25 K between the rSOC reactor and heat storage would result in a temperature difference of 50 K between SOFC operation temperature and SOEC operation temperature. At a reactor temperature of 850 °C in SOFC mode and 1 bar pressure, the roundtrip efficiency increased from 56% to 58% when ΔT was reduced from 25 to 10 K. Therefore, to achieve higher efficiencies, the rSOC reactor operation temperature in the SOFC and SOEC mode should be as close as possible.

Impact of Operation Current Density: The effect of current density is shown in **Figure 5**. The impact of current density on the rSOC system performance is straightforward. The voltage losses are a product of current density and ASR. Hence, at lower current densities, the losses are reduced. Therefore, the work output from the rSOC reactor in SOFC mode is higher and work input to the rSOC reactor in SOEC mode is reduced. This leads to higher roundtrip efficiencies at lower current densities. In contrast, for a give power demand, lower current densities require large reactor areas thereby increasing the cost.

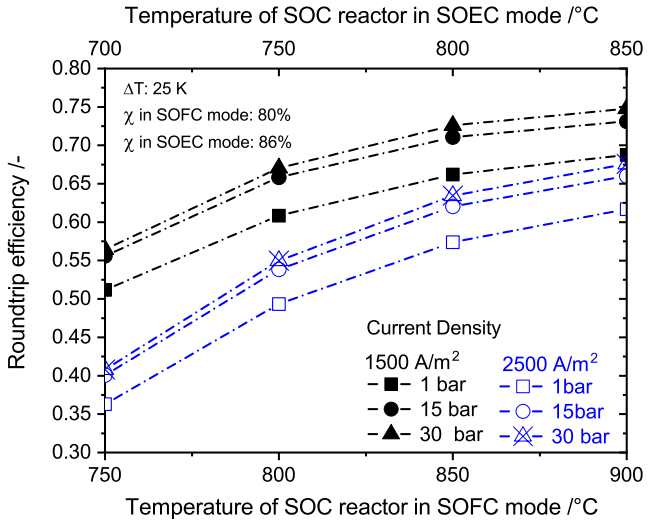

Figure 5. Impact of current density on roundtrip efficiency for the system with commercial reactor, conversion (χ) = 86% in SOEC mode. $T_{fc} - T_{ec} = 2\Delta T$.

2.4. Summary

From the theoretical and experimental analysis, it can be observed that the reactor performance has a significant impact on the efficiency. The theoretical maximum roundtrip efficiency (ideal) that can be attained for the proposed concept is close to 98%. The impact of the reactor performance limits the achievable efficiency to 55–65%. Therefore, the selection of the reactor operation parameter is critical for the system performance. On the basis of the results, the average operation temperature of the reactor should be in the range of 800–850 °C and operation temperature in both modes should as close as feasible. A higher operation pressure is preferred as it leads to higher efficiency and also leads methane within the rSOC reactor during the electrolysis operation. For the process system analysis, a operation pressure of 25 bar is chosen. The methane content in rSOC product during the electrolysis is less than 20 mol% at these pressures and temperature. Therefore, an additional downstream methanation process is required for increasing the methane concentration required for gas grids. An operational current density of 2500 A m^{-2} is chosen.

3. Process System Analysis

In this section, based on the theoretical and experimental study, a process system analysis performed. A system configuration is defined to achieve the efficiency predicted in the previous section. Unlike in the theoretical evaluation, for the process system simulation, realistic constraints have to be considered. The losses due to heat and mass transport, irreversibilities in the BoP components should be considered. The process system simulation is implemented in Aspen Plus chemical process engineering software. The description of the components is provided in the Supporting Information. The models for heat exchangers, pumps, and other BoP were obtained for model library available in Aspen Plus. The heat storage model in Aspen Plus was implemented as proposed by Mottaghizadeh et al.[25] The chemical reactor models for methanation reactors were implemented assuming chemical equilibrium using the "RGIBBS" model in Aspen Plus. Finally, the validated 1-D rSOC reactor model was used for system simulation, and for further details, refer to Srikanth et al.[29] The 1-D rSOC reactor models the global electrochemical reaction using the Butler–Volmer kinetic models. The electrochemical parameters required for the model were obtained from experimental results presented in detail by Riedel et al.[35] The mass transport between within the porous electrodes were modeled using multi-component dusty gas model (DGM). Finally, in the model, the key properties (temperature, compositions, current densities, etc.) were resolved along the flow direction, assuming the reactor to be a plug flow reactor. The model used assumes a lumped temperature along the height of the anode–electrolyte–cathode layer. The 1-D rSOC reactor model was validated with a commercially available electrolyte supported cell (ESC) design rSOC reactor with ten cells. The rSOC reactor has a coflow configuration with an open-air electrode design. The electrolyte is made of 3YSZ with a thickness 90 μm. The fuel electrode is 30 μm made of nickel–gadolinum-doped ceria (Ni-GDC) cermet. The air electrode is composed of LSCF with a thickness of 30 μ. A detailed description of the stack is provided by Riedel et al.[35] The validated model is flexible and can be used to simulate reactors with any number of cells or reactor modules with many reactors each containing more 60...120 cells. The simplified process flow diagram of the methane-based gas-grid-connected rSOC system is shown in **Figure 6**. The SOFC and SOEC process are described in Figure 6a,b respectively. A brief description of the process in both SOFC and SOEC mode is described later.

3.1. Process Description

3.1.1. SOFC Operation Mode

Methane from the natural gas grid is supplied as fuel to the rSOC system during the SOFC operation. It is assumed that the fuel is supplied to the system at the operational pressure of 25 bar. It is mixed with the fuel exhaust recycle stream which is at a higher temperature. The fuel exhaust stream of the rSOC reactor consists mainly of steam and carbon-dioxide. Steam is required to be added to the fuel for the steam reforming reaction to take place in the prereformer. Also, steam is added to the fuel stream to increase the O/C ratio prevent carbon deposition in the system. A steam-to-carbon ratio (STCR) of 2 or above is typically recommended.[38,39] The resulting fuel mixture is then preheated in the heat recovery units and fed to the prereformer where the methane undergoes steam reforming. The reformate product gas has a lower temperature at the outlet due to the endothermic reforming reaction. It is then fed to the final heat recovery unit where it is heated to the required fuel inlet temperature of the rSOC reactor during the SOFC operation. Air is supplied to the system from the ambient and is compressed to the system pressure of 25 bar. It is then preheated in the heat recovery units and mixed with the air exhaust recycle stream. The recycle ratio is determined such that the air mixture temperature achieves the inlet temperature required for the rSOC reactor during SOFC operation. The product gas from the SOFC exhaust mostly consists of H_2O, CO_2, and unconverted H_2 and CO. The air and fuel exhaust streams from the rSOC reactor are sent to heat storage unit, where the heat produced in the rSOC reactor is stored. Heat storage was shown to be beneficial for thermal management of rSOC system by Mottaghizadeh et al.[25] Remaining heat in the exhaust streams are used for preheating the inlet streams in the heat recovery unit and part of the fuel exhaust stream is recycled to the inlet. The fuel exhaust stream is further cooled to condense and remove the water. The remaining CO_2 and the unreacted CO and H_2 is fed to the exhaust tank.

3.1.2. SOEC Operation Mode

During the SOEC process, H_2O and CO_2 is fed to the rSOC reactor for coelectrolysis. The CO_2 required for coelectrolysis is obtained from the gas stored in the exhaust tank during the SOFC operation. The mass flow rates of H_2O and the exhaust gas mixture are chosen such that H/C ratio is equal to 7 required for high methane production.[30] Water is first pumped to the system operational pressure of 25 bar. It is then fed to the steam generation unit which is coupled to the methanation reactor unit.

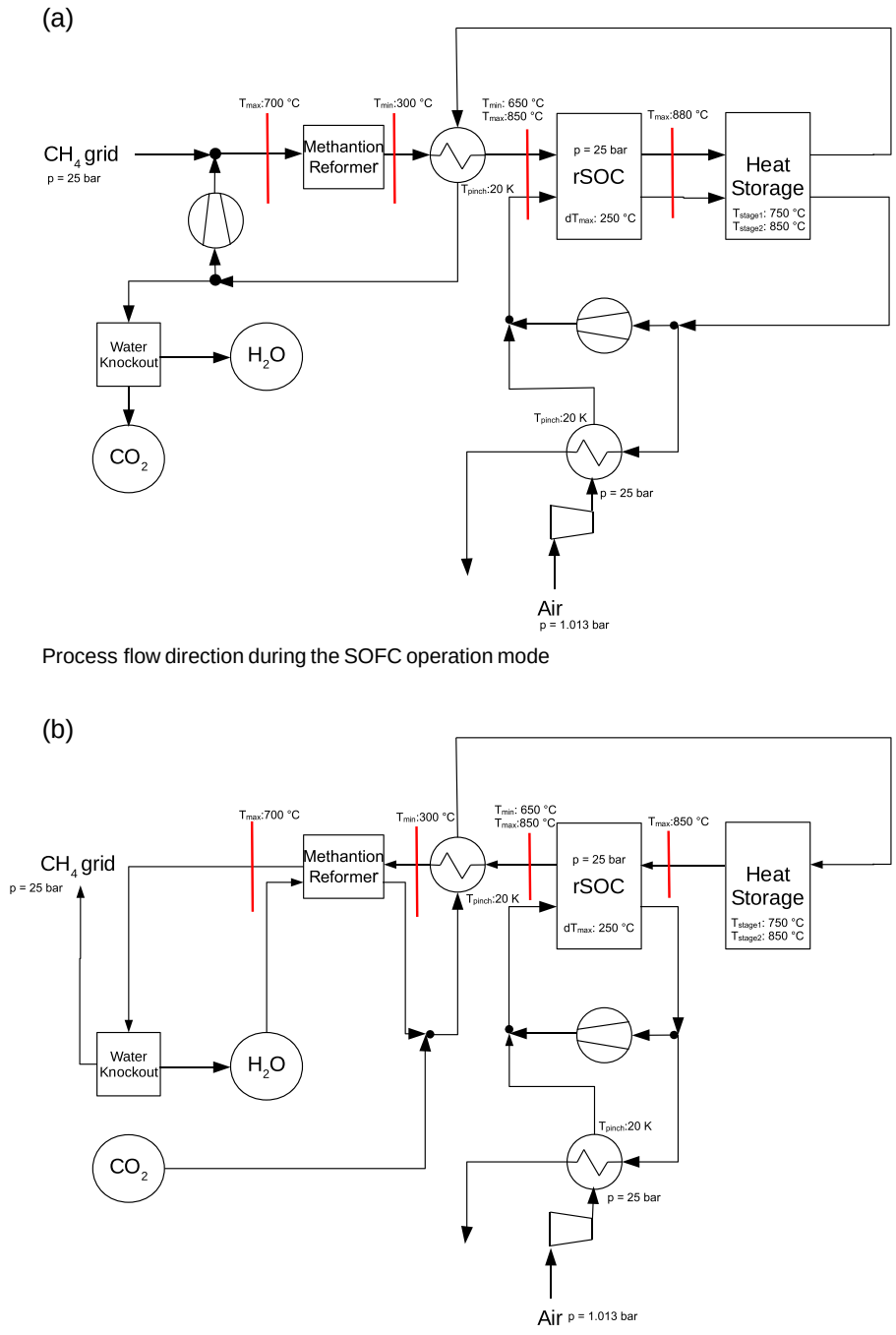

Figure 6. Process flow diagram of the methane-based gas grid connected rSOC system.

Heat produced during the exothermic methanation downstream process is used for steam generation. The produced steam is then fed to the final heat recovery unit and mixed with the CO_2-dominated exhaust gas mixture which is preheated in the heat recovery unit. The CO_2-dominated exhaust gas mixture contains some amount of H_2 required to prevent oxidation of Ni in the fuel electrode. The mixture of steam, carbon dioxide, and hydrogen is then passed through the heat storage units where it absorbs the heat stored during the SOFC operation and later enter the rSOC reactor. Air is first compressed to the system pressure and preheated in the heat recovery unit. An air exhaust recycle unit is used for the SOEC process as well. The preheated air is then mixed with the air exhaust recycle stream. After the electrolysis, the fuel gas (syngas) produced by the rSOC reactor is cooled to a temperature of 300 °C and fed to the downstream process. A methanation process is used for the downstream process.

The final fuel with high methane content is separated from the water. The synthetic natural gas should be further processed to increase the Wobbe index as per requirements before it is fed to the gas grid. The air exhaust from the rSOC reactor is partly recycled and cooled in the heat recovery unit. It is then expanded to the atmospheric pressure before released to the environment.

3.2. Boundary Conditions and Constraints

For the system simulation, certain boundary conditions and constraints considered for the modeling. A common set of constraints were defined for the rSOC reactor, methanation/reformer unit, and heat storage tanks during SOFC and SOEC operation modes. The boundary conditions and constraints for the different components during different operation modes are given in **Table 1**. A conscious effort was made to keep the effective (or average) rSOC reactor temperature at 800 °C or above.The other parameters such as the inlet temperatures to rSOC reactor were varied accordingly based on performance, boundary condition constraints, reactor safety, and feasibility.

3.3. Results and Discussion

The energy flows in the system during SOFC and SOEC operation mode are depicted in form of Sankey diagrams. The energy flows are normalized by dividing them by the chemical energy supplied to the system in SOFC operation or produced by the system in SOEC operation. The chemical energy produced by the system in the SOEC operation mode is equal to the chemical energy supplied to the system in the SOFC operation mode. The performance of the methane-based rSOC system in SOFC and SOEC operation mode is summarized in **Table 2**. The reactor roundtrip efficiency of 62.2% and the net system roundtrip efficiency of 52.9% was achievable for the rSOC system. The lower system roundtrip efficiency as compared to the reactor roundtrip efficiency is due to the high parasitic work consumption in BoP components.

Table 1. Boundary conditions and constraints for the methane-based rSOC system.

Parameters	Value	Unit
System pressure	25	bar
rSOC reactor	–	–
Fuel inlet temperature	650–850	°C
Air inlet temperature	650–850	°C
Maximum temperature difference	250	°C
Maximum outlet temperature	880	°C
Single pass reactant conversion	85–95	%
Operation current density	2500	A m^{-2}
Heat storage unit		
Stage 1 storage temperature	850	°C
Stage 2 storage temperature	750	°C
Pinch point	5	K
Methanation and reforming	–	–
Minimum temperature	300	°C
Maximum temperature	700	°C
Heat exchangers	–	–
Pinch point	20	K

Table 2. Performance of the methane-based rSOC system at a current density of 2500 A m^{-2}.

Parameter	Value	Unit
SOFC operation mode	–	–
Average reactor temperature	845	°C
Average reactor voltage	0.772	V
Net efficiency in SOFC mode	57	%
SOEC operation mode	–	–
Average reactor temperature	800	°C
Average reactor voltage	1.235	V
Net efficiency in SOEC mode	92.9	%
Roundtrip efficiency		
Reactor (gross)	62.2	%
System (net)	52.9	%

3.4. Overview of System Performance

3.4.1. Performance in SOFC Operation Mode

The Sankey diagram of the energy flows in the system is shown in **Figure 7**. During the SOFC operation mode, methane is supplied to the system from the gas grid and corresponds to 100% of the chemical energy supplied. It is mixed with the fuel exhaust recycle stream obtained from the rSOC exhaust stream. The temperature of the fuel exhaust recycle stream is 678 °C. A recycle ratio (defined by ratio of mass flow rate in recycled steam to total mass flow leaving the rSOC reactor) of 0.48 is required to achieve the required STCR to avoid carbon deposition in the pipe, reformer, and the rSOC reactor. The exhaust recycle stream contains 8.8% of the chemical energy supplied to the system. It also

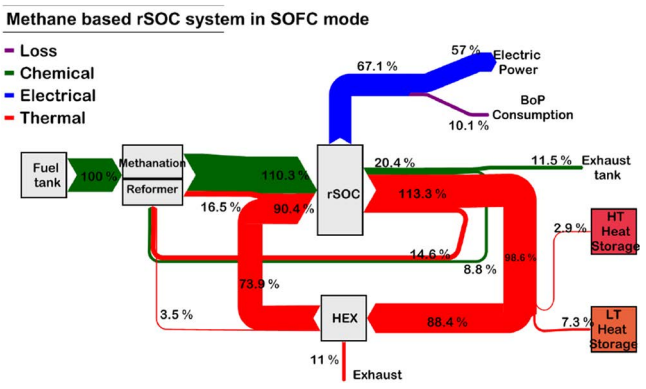

Figure 7. Chemical, electrical, and thermal energy flows represented in Sankey diagram for the methane-based rSOC system at 2500 A m^{-2} in SOFC operation mode. All flows are normalized by dividing by the chemical energy input to the system.

transmits thermal energy equivalent to 14.6% of the chemical energy supplied to the system due to its high temperature. The resulting fuel mixture is at a temperature of 459 °C and is preheated to 670 °C in the heat recovery unit where it absorbs thermal energy equal to 3.5% of the chemical energy supplied to the system. It is then fed to the prereformer unit where it is prereformed. The reformate gas exits the prereformer at a temperature of 594 °C. The lower outlet temperature is due to the endothermic reforming reaction. The chemical energy of the reformate is increased to 110% of the chemical energy supplied to the system. It is then preheated to the required fuel inlet temperature of 750 °C. Air required for the SOFC operation is compressed to 25 bar from the ambient. The compressed air is then preheated in the heat recovery unit and mixed with the air exhaust recycle stream. An air exhaust recycle ratio of 0.48 was required to increase the temperature of the air mixture to the required inlet temperature of 700 °C. The reactants entering the rSOC reactor carry 90.4% of the chemical energy supplied to the system as thermal energy. During the SOFC operation, the variation of temperature and voltage loss along the length of the rSOC reactor is shown in **Figure 8** for the rSOC inlet conditions and operation parameters. A drop in reactor is observed near the inlet of the rSOC reactor. This temperature reduction is due to the endothermic steam reforming reaction of the remaining methane in the inlet feed which occurs close to the reactor inlet. The local temperature increases along the reactor length due to exothermic reaction and heat due to the losses. The local thermodynamic voltage of the reactor decreases along the reactor length due to decreasing concentration of fuel components (H_2 and O_2) and increasing temperature along reactor length. The voltage loss also decreases along the reactor length. This is due to decreasing ASR with higher temperature toward reactor outlet and also due to decreasing local current density along the length of the reactor. The local current density is the measure of local rate of electrochemical reaction. At the inlet, the driving for the reaction is higher (indicated by local thermodynamic voltage) leading to higher current density near the inlet. Toward the outlet, most of the reactants are consumed, thereby reducing the driving force for the reaction and hence rate of electrochemical reaction is lower. The combination of high local current density, lower reactor temperature, and high ASR near the reactor inlet leads to high exergy losses. The rSOC reactor operates at a cell voltage of 0.773 V. The gross electrical energy produced by the rSOC reactor in SOFC operation amounts to 67% of the chemical energy supplied to the system. This corresponds to the gross electrical efficiency of the system in SOFC operation. Electrical energy equalling 10% of the chemical energy supplied to the system is consumed by the BoP components. Hence, a net electrical efficiency of 57% is achieved in SOFC operation of the rSOC system. The thermal energy generated in the rSOC reactor accounts for 23% of the chemical energy input to the system. The heat generated in the rSOC reactor is carried by the product streams leaving the rSOC reactor. Hence, the thermal energy of the product stream is increased to 113% of the chemical energy supplied to the system. The fuel exhaust stream contains 20.4% of the initial chemical energy fed to the system. The heat stored in the thermal energy storage system accounts for only 10% of the input chemical energy. The remaining thermal energy in the exhaust streams is used to the preheat in the inlet reactants. The fuel exhaust stream is cooled in water knockout unit, where CO_2, unreacted H_2, and CO are separated from water and sent to the exhaust tank. The fuel exhaust stream fed to the exhaust tanks contains chemical energy equal to 11.5% of the chemical energy supplied to the system.

3.4.2. Performance in the SOEC Operation Mode

The energy flows for the rSOC system in SOEC operation mode is shown in **Figure 9**. The energy flows are normalized by dividing by the chemical energy produced by the system. In the SOEC operation mode, the mixture of H_2O and CO_2 is fed to the rSOC reactor as reactant. The reactant mixture also contains some amount of H_2 and CO. Therefore, it possesses chemical energy equalling 11.7% of the chemical energy produced by

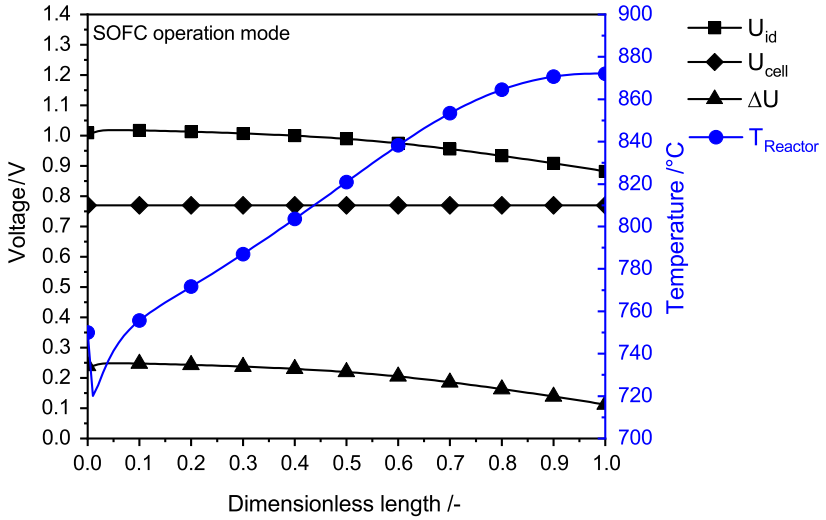

Figure 8. Variation of temperature, ideal voltage, and losses along the length of single repeat unit at system operation conditions at an average current density at 2500 A m^{-2} in SOFC operation mode.

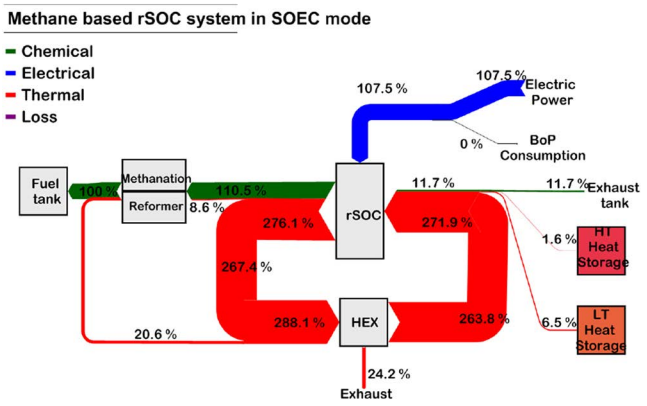

Figure 9. Chemical, electrical, and thermal energy flows represented in Sankey diagram for the methane-based rSOC system at 2500 A m^{-2} in SOEC operation mode. All flows are normalized by dividing by the chemical energy input to the system.

the system. The water supplied to the system from the water tank is pumped to the system pressure of 25 bar before it is fed to the steam generation unit. The steam generation unit is interlinked with the downstream methanation process. As the methanation process is exothermic, the heat produced during the methanation process is utilized for the steam generation. The methanation process generates 20.6% of the chemical energy produced by the system as thermal energy. This thermal energy is used for steam generation. A superheated steam at a temperature 480 °C is obtained at the outlet of the steam generator. The CO_2 exhaust mixture from the exhaust tank is preheated to around 325 °C and mixed with the steam. The gas mixture is then passed through the heat storage units where it is brought to the inlet temperature of 785 °C in SOEC operation mode. Air is fed the system as sweep gas and also as heat transfer media is compressed to the system pressure of 25 bar from ambient conditions. The compressed air is preheated in the heat recovery unit and mixed with the air from the exhaust recycle unit. The air mixture is then supplied to the rSOC reactor at a temperature of 785 °C. The air and reactants entering the rSOC reactor posses thermal energy equal to 272% of the chemical energy produced by the system. The total heat absorbed by the reactant mixture and air from the heat storage unit accounted for 8% of the chemical energy produced by the system. The first stage contributed 1.6% and second contributed 6.5% of the chemical energy produced by the system as heat. The variation of temperature, thermodynamic voltage, and voltage losses for the rSOC reactor during the SOEC operation is shown in **Figure 10**. The reactor temperature initially decreases due to the strong endothermic electrochemical reaction and heat due to losses is not sufficient to balance the heat demand of the reaction. Toward the end of the reactor, the temperature increases. This is due to the rate of exothermic internal methanation reaction that occurs toward the reactor outlet. As H_2 and CO are produced from electrochemical reaction, the conditions become favorable for methanation reactor toward the reactor outlet. The heat from exothermic methanation reaction coupled to heat due to losses results in a slightly exothermic electrolysis operation. The fuel and air product streams exit the rSOC reactor with a temperature 810 °C. The local thermodynamic voltage gradually increases along the reactor length due to increasing concentration of fuel components (H_2, CO, and O_2) toward the reactor outlet. The local voltage loss decreases along the reactor length. This is due to the increase in temperature along the reactor length which lowers the local ASR and also the decreasing local current density similar to that of the SOFC process. The rSOC reactor consumes 107.5% of the chemical produced by the system as electrical energy. The BoP electrical energy consumption is insignificant and hence electrical energy consumption of the reactor represents the net electrical energy consumption of the system. The rSOC reactor operates at a cell voltage of 1.235 V producing a syngas mixture with a 16 mol% of methane at the rSOC outlet. The chemical energy of the syngas mixture is 110% of the chemical energy produced by the system. The thermal energy of the product stream from

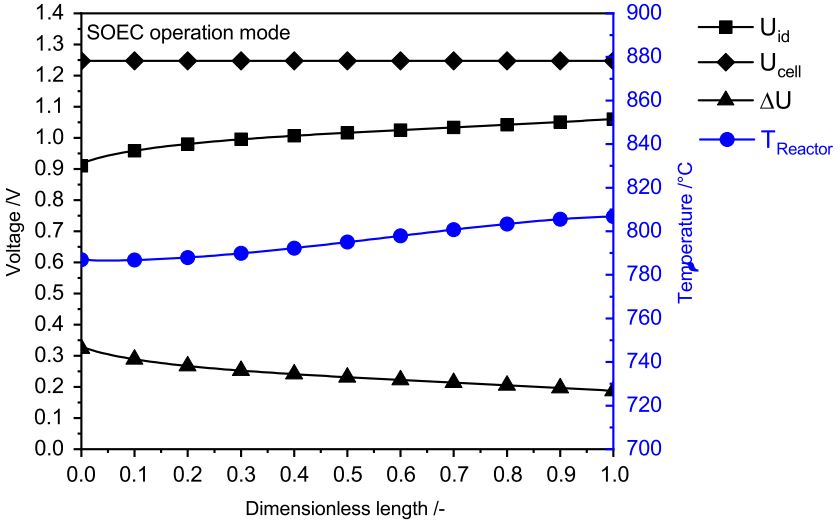

Figure 10. Variation of temperature, ideal voltage, and losses along the length of the single repeat unit at system operation conditions with current density at 2500 A m^{-2} in SOEC operation mode.

the rSOC reactor increased by 5–276% of the chemical energy produced by the system. This is due to the exothermic SOEC operation of the rSOC reactor. The syngas mixture is then processed in the downstream methanation process. It is first cooled to 300 °C to be fed to the methanation process. The syngas mixture undergoes the methanation process through a cycle of intercooling between the different stages of the methanation process. The final product gas exits the methanation unit with a temperature of 335 °C and is then cooled to remove the water from the fuel stream. The final fuel gas contains 92 mol% of CH_4, 7 mol% of H_2, and traces of CO_2 and CO. At the end of the methanation process, the produced fuel lost 10.5% of chemical energy in the raw syngas from the rSOC reactor and the chemical energy of the final product fuel is 100%. The lost chemical energy from the syngas is converted to heat during the exothermic methanation reactions. Part of the air at the outlet of the rSOC reactor is recycled back to the inlet. The remaining air is then cooled in the heat recovery unit and then finally expanded to the ambient pressure to extract work. A net efficiency (chemical to electricity) of 93% was achieved for the rSOC system in SOEC operation.

3.4.3. Effect of Heat Storage Units for Thermal Management

Despite the exothermic behavior of the rSOC reactor in electrolysis operation and exothermic downstream methanation process, thermal energy is consumed from the heat storage tanks during the SOEC operation mode. The thermal energy consumption from the storage tanks is equal to 8% of the chemical energy produced during the SOEC operation mode. The thermal energy from the heat storage is used for the process heating purposes to raise the process streams entering to the rSOC reactor to the required inlet temperature in the SOEC mode. In the absence of a heat storage system, the equivalent heat has to be supplied via external means such as an electrical heater or combustion of part of the methane produced in the SOEC mode. This will reduce the system efficiency during the SOEC operation to 86% and thereby reduce the roundtrip efficiency to 49%. Therefore, using the heat storage method for thermal management, the heat produced during the SOFC operation was stored and utilized for process heating during the SOEC operation mode. This yielded an increase in roundtrip efficiency of 4% points. Therefore, it is shown from a process system perspective that the thermal management using a heat storage can aid in improving the system performance of a methane-based rSOC system as concluded by Mottaghizadeh et al.[25] Consequently a techno-economic analysis is required to further justify whether the 4% points increase in system performance using the heat storage is justifiable from an economic perspective.

3.4.4. Exergy Analysis

An exergy analysis is performed to identify the areas of entropy generation and opportunities to optimize the system performance. The contribution of losses from different components to the total exergy loss in SOFC and SOEC operation mode is shown in **Figure 11**.

SOFC Operation Mode: The contribution of the key system components to the total exergy destruction is calculated to identify the major source of entropy production. The rSOC reactor contributed almost 43% of the total exergy loss in the system. This can be greatly reduced by improving the reactor performance and reducing the electrochemical losses in the reactor. Additionally, this can also be improved by matching the high local temperature with high local current density within the reactor. This would lead to lower voltage losses and hence lower exergy loss in the reactor. It was closely followed by the exergy losses in the heat recovery unit with 34%. In the evaluation of the exergy losses in the heat recovery unit, the exergy destruction due to the mixing of the cold methane fuel with the recycled hot SOFC product gas is included. This contributed majorly to the high exergy losses in the heat recovery unit. To reduce this exergy destruction, the temperature difference between the two streams should be as small as possible. The air compressor and air expander contributed up to 12% and 8% of the total exergy loss during the SOFC operation mode. The exergy losses due to the air compressor and expander can be greatly reduced by considering an pressurized air storage tank as proposed by Mottaghizadeh et al.[25]

SOEC Operation Mode: In the SOEC operation mode, similar to the SOFC operation mode, the rSOC reactor contributed

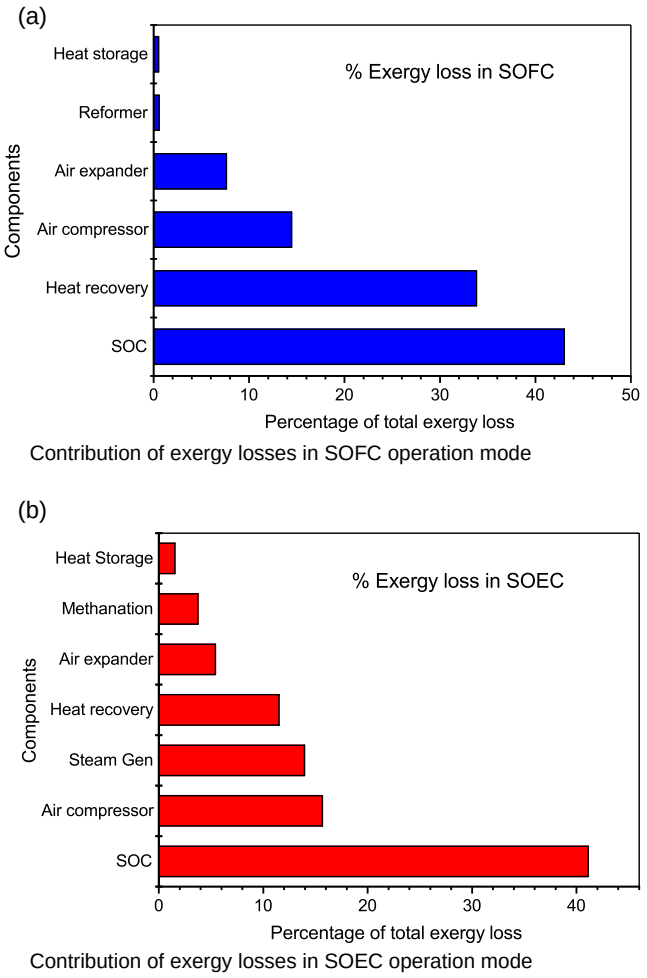

Figure 11. Contribution of different system components to the total exergy loss in the rSOC system for a) SOFC operation mode and b) SOEC operation mode.

approximately 41% of the total exergy loss which is due to the electrochemical losses in the reactor. From process system perspective, the exergy loss in the rSOC can be addressed by raising the average operation temperature of the reactor by optimizing the system parameters. Alternatively, the electrochemical losses can be reduced by cell optimization. The exergy destruction occurs in the air compressor at around 14% of the total exergy loss which can be avoided using a pressurized air storage tank. Steam generation is critical in the SOEC process. In the proposed system, high-temperature heat from methanation process and outlet gases from the SOC reactor were used as heat source for steam generation. The heat sources are at a temperature of 400–600 °C, whereas the steam generation occurs at 225 °C at 25 bar. This temperature difference in the heat transfer results in the high exergy destruction observed in the steam-generation process. The exergy losses in steam generation accounted for 18% of the total exergy loss. The exergy losses in heat recovery unit is equal to 14% of the total exergy loss. The contribution of the heat recovery unit to exergy loss in SOEC operation mode is considerably less than in the SOFC operation as there is no hot fuel recycle mixing with a cold inlet reactant during SOEC operation. The air expander, methanation reactor, and heat storage contributed to 6%, 4%, and 2% of the total exergy losses, respectively. The exergy losses in the methanation system are due to the exothermic nature of the reaction and due the chemical reaction itself.

4. Conclusions

A process system study of a methane-based energy conversion system for energy storage and sector coupling using a commercially available rSOC reactor was performed. The proposed process system is especially attractive as it can provide electrical grid arbitration by producing electricity when gas price is low and vice versa, link electrical energy industry with chemical process industry, and the methane produced can be directly supplied to the natural gas grid without the need for storage tanks. Reznicek[40] showed in their detailed techno-economic analysis that cost of storage can be as high 32% of the total capital cost. By supplying the product gas directly to the natural gas grid, the capital cost associated with the storage tanks can be reduced. Additionally, by interacting with the gas grid, the storage capacity is not limited by the tank sizing. A detailed techno-economic analysis of the proposed system is required to completely quantify the economic benefits of avoiding the storage tanks. In this work, pressurized operation was shown to be beneficial for the SOC reactor and also to enable higher system efficiency and methane production by the adopted methodology. The pressurized operation of an electrolyte-supported design SOC reactor was shown to be technically feasible in the HELMETH EU project where SOC reactor and coelectrolysis system demonstrated at 15 bar pressure.[41,42] Though further R&D and engineering studies are required to ensure feasiblity for long-term operation and further reduction in costs. A summary of the key results are as follows: 1) The adopted methodology assisted in quickly narrowing down the preferred operation points of the system based on the reactor performance by combining theoretical and experimental methods. An efficiency target based on thermodynamics and limitations of the rSOC reactor was determined. 2) For the proposed concept based on a commercial rSOC reactor, the maximum energy storage efficiency that is feasible in between 55% and 65%. Energy storage efficiency of 63% is feasible at operation temperature of 850 °C, pressure of 20 bar, and average current density of 2500 A m^{-2}. 3) A process system design and analysis was performed to quantify the achievable efficiency for a complete system including BoP. A chemical–electrical conversion efficiency of 57% can be achieved in the SOFC operation mode and an electrical–chemical conversion efficiency of 93% can be achieved in SOEC operation mode. A net electrical storage efficiency of 53% was reached. The energy storage efficiency of the complete process system is 10% less than the maximum value feasible for the given rSOC reactor. This is due to parasitic consumption in BoP. Energy storage efficiencies as high as 73%[43] by storing methane in tanks were achieved. Similarly, roundtrip efficiency of 40%[44] were reported by for rSOC system where methane was supplied to the grid. A roundtrip efficiency of 53% was shown to be feasible by Wang et al. with hydrogen as a storage medium using 3-D rSOC reactor model.[45] It should be noted that these studies were based on rSOC reactors that are in early stages of development and not commercially available. In this study, a commercially available state-of-the-art reactor was used, and using similar reactor, Mottaghizadeh et al.[25] reported a roundtrip efficiency of 60% by storing methane and compressed air in pressurized storage tanks. 4) The design process system produces a fuel mixture with 92 mol% of the methane (CH_4) during the electrolysis process. 5) Heat storage for thermal management is beneficial for system performance. Without this, the net storage efficiency reduces by 4% points. Techno-economic analysis is required to justify the benefits against economic costs. 6) An exergy analysis was performed. The rSOC reactor was the major contribution to exergy loss in both SOFC and SOEC mode. An optimization effort should focus on improving the reactor performance and reducing exergy losses in the heat recovery unit.

Supporting Information

Supporting Information is available from the Wiley Online Library or from the author.

Acknowledgements

This work was partially supported by Deutscher Akademischer Austauschdienst (DAAD)

Conflict of Interest

The authors declare no conflict of interest.

Keywords

energy storage, power to gas, reversible solid oxide cells

Received: May 26, 2019
Revised: December 22, 2019
Published online:

[1] R. M. Dell, *J. Power Sources* **2001**, *100*, 2.
[2] H. Chen, T. N. Cong, W. Yang, C. Tan, Y. Li, Y. Ding, *Progr. Nat. Sci.* **2009**, *19*, 291.
[3] A. Sternberg, A. Bardow, *Energy Environ. Sci.* **2015**, *8*, 389.
[4] K. Hemmes, J. M. Guerrero, T. Zhelev, *Chem. Eng. Process. Process Intens.* **2012**, *51*, 18.
[5] L. Mingyi, Y. Bo, X. Jingming, C. Jing, *J. Power Sources* **2008**, *183*, 708.
[6] M. Henke, C. Willich, J. Kallo, K. A. Friedrich, *Int. J. Hydrog. Energy* **2014**, *39*, 12434.
[7] F. Muellerlanger, E. Tzimas, M. Kaltschmitt, S. Peteves, *Int. J. Hydrog. Energy* **2007**, *32*, 3797.
[8] Q. Fu, C. Mabilat, M. Zahid, A. Brisse, L. Gautier, *Energy Environ. Sci.* **2010**, *3*, 1382.
[9] W. Li, H. Wang, Y. Shi, N. Cai, *Int. J. Hydrog. Energy* **2013**, *38*, 11104.
[10] C. Graves, S. D. Ebbesen, M. Mogensen, *Solid State Ion.* **2011**, *192*, 398.
[11] D. M. Bierschenk, J. R. Wilson, S. A. Barnett, *Energy Environ. Sci.* **2011**, *4*, 944.
[12] S. Santhanam, M. P. Heddrich, M. Riedel, K. A. Friedrich, *Energy* **2017**, *141*, 202.
[13] N. Aldag, **2016**. http://www.sunfire.de/en/company/press/detail/sunfire-supplies-boeing-with-worlds-largest-commercial-reversible-electrolysis-rsoc-system-16.
[14] J. Mermelstein, O. Posdziech, *Fuel Cells* **2017**, *17*, 562.
[15] M. Gassner, F. Maréchal, *Energy* **2008**, *33*, 189.
[16] R. R. Dickinson, D. L. Battye, V. M. Linton, P. J. Ashman, G. G. J. Nathan, *Int. J. Hydrog. Energy* **2010**, *35*, 1321.
[17] W. L. Becker, M. Penev, R. J. Braun, *J. Energy Resour. Technol.* **2019**, *141*, 021901.
[18] E. Giglio, F. A. Deorsola, M. Gruber, S. R. Harth, E. A. Morosanu, D. Trimis, S. Bensaid, R. Piron, *Ind. Eng. Chem. Res.* **2018**, *57*, 4007.
[19] L. Wang, J. Düll, F. Maréchal, *Int. J. Hydrog. Energy* **2018**, *44*, 9529.
[20] C. Bang-Møller, M. Rokni, *Energy Convers. Manage.* **2010**, *51*, 2330.
[21] V. Verda, M. C. Quaglia, *Int. J. Hydrog. Energy* **2008**, *33*, 2087.
[22] C. Haynes, *J. Energy Resour. Technol.* **2002**, *124*, 95.
[23] A. Monti, C. Wendel, M. Santarelli, R. J. Braun, *ECS Trans.* **2015**, *68*, 3289.
[24] C. H. Wendel, P. Kazempoor, *J. Power Sources* **2015**, *276*, 133.
[25] P. Mottaghizadeh, S. Santhanam, M. P. Heddrich, K. A. Friedrich, F. Rinaldi, *Energy Convers. Manage.* **2017**, *142*, 477.
[26] M. Li, J. Brouwer, A. D. Rao, G. S. Samuelsen, *J. Power Sources* **2011**, *195*, 5903.
[27] L. Magistri, R. Bozzo, P. Costamagna, A. F. Massardo, *J. Eng. Gas Turbines Power* **2004**, *126*, 516.
[28] N. F. Harun, L. Shadle, D. Oryshchyn, D. Tucker. in *Turbo Expo 2017: Turbomachinery Technical Conference and Exposition*, ASME, Charlotte, NC **2017**. p. V003T06A020.
[29] S. Srikanth, M. Heddrich, S. Gupta, K. Friedrich, *Appl. Energy* **2018**, *232*, 473.
[30] J. Gao, Y. Wang, Y. Ping, D. Hu, G. Xu, F. Gu, F. Su, *RSC Advances* **2012**, *2*, 2358.
[31] J. Mermelstein, M. Millan, N. Brandon, *J. Power Sources* **2010**, *195*, 1657.
[32] M. Liu, M. G. Millan, P. V. Aravind, N. Brandon, *J. Electrochem. Soc.* **2011**, *158*, B1310.
[33] K. Girona, J. Laurencin, J. Fouletier, F. Lefebvre-Joud, *J. Power Sources* **2012**, *210*, 381.
[34] M. Liu, P. V. Aravind, T. Woudstra, V. R. M. Cobas, A. H. M. Verkooijen, *J. Power Sources* **2011**, *196*, 7277.
[35] M. Riedel, M. Heddrich, K. Friedrich, *Int. J. Hydrog. Energy* **2019**, *44*, 4570.
[36] S. K. Ratkje, S. Møller-Holst, *Electrochim. Acta* **1993**, *38*, 447.
[37] S. L. Miller, M. N. Svrcek, K. Y. Teh, C. F. Edwards, *Energy* **2011**, *36*, 99.
[38] N. Autissier, F. Palazzi, F. Marechal, J. van Herle, D. Favrat, *J. Fuel Cell Sci. Technol.* **2007**, *4*, 123.
[39] J. Van Herle, F. Maréchal, S. Leuenberger, D. Favrat, *J. Power Sources* **2003**, *118*, 375.
[40] E. Reznicek, *Energy Convers. Manage.* **2018**, *175*, 263.
[41] J. Brabandt, O. Posdziech, *ECS Transact.* **2017**, *78*, 2987.
[42] M. Landgraf, C. P. Officer, Press Release, Karlsruhe Institute of Technology, Karlsruhe **2014**.
[43] C. H. Wendel, P. Kazempoor, R. J. Braun, *J. Power Sources* **2016**, *301*, 93.
[44] B. Chen, Y. S. Hajimolana, V. Venkataraman, M. Ni, P. Aravind, *Appl. Energy* **2019**, *250*, 558.
[45] Y. Wang, A. Banerjee, L. Wehrle, Y. Shi, N. Brandon, O. Deutschmann, *Energy Convers. Manage.* **2019**, *196*, 484.